# Mechanical Property of Dissimilar Material Nanocomposites Prepared by Ion Beam Assisted Sputtering Process †

Jianli HE*, Yuichi SETSUHARA**, Ippei SHIMIZU***, Shoji MIYAKE****

## Abstract

*To study the property tailoring effect of dissimilar material composites, Ti-B-N films were synthesized by an ion beam assisted sputtering system. Structural analysis and mechanical property evaluation were carried out to check whether or not the presence of h-BN in $TiB_2$-based material is capable of producing better anti-wear performance. The Ti-B-N films were found to have a structure which comprised nanosized $TiB_2$ and TiN crystallites and a thin layer matrix of hexagonal boron nitride. Compared with pure $TiB_2$, improved tribological properties were observed for the Ti-B-N films. Bombarding energy and substrate temperature were found to have great influence on the film properties. When the bombarding energy was around 150eV and the growth temperature was about 100°C, the wear rate of Ti-B-N film was about two orders lower than that of pure $TiB_2$ film. Also, films synthesized under this condition displayed higher load-bearing capacity and smaller friction coefficient.*

## 1. Introduction

The concept of property tailoring by dissimilar material combination is important, especially for protective surface coatings. This is because wear-resistance is influenced not only by the hardness but also by many other properties like coefficient of friction, toughness, etc. It is rare for a single pure material to meet all these requirements at the same time, for example, superhard materials are usually brittle and lubricating materials are often soft. Therefore, when such materials of contrary properties are combined together, it is reasonable to expect some optimization and correspondingly better anti-wear performance. In the literature, there were reports of improvement of anti-wear performance by incorporating soft lubricating materials(C, $MoS_2$) into hard materials(TiN, $TiB_2$).[1,2] Particularly, if the grain size of such a composite is on the nanometer scale, extra profit can be possible due to the hardness enhancement.[3,4]

In this regard, the Ti-B-N system is interesting because there exist several phases of contrary properties, i.e., hard phases (TiN, $TiB_2$, c-BN) and soft phases(h-BN). In the

past, researches concerning the Ti-B-N system were mainly directed to obtain superhardness. On the contrary, much less attention was paid to the application study of hexagonal BN which was once evaluated as a potential solid lubricant.[5,6] This is partly because h-BN was reported to have a high friction coefficient and was thus assumed as inferior to other lamellar structures such as graphite and molybdenum disulfide($MoS_2$).[7,8] However, when appropriately integrated with $TiB_2$ or c-BN, the lamellar nature of h-BN makes it possible to annihilate the common severe compressive stress, decrease the friction and, as a result of property tailoring effect, improve the overall tribological performance. Unfortunately, there have been few reports on this issue.

In this work, we synthesized composite coatings in the Ti-B-N system by a dual ion beam equipment. The tribological properties were specifically studied to determine whether or not the presence of h-BN is capable of producing better anti-wear performance. Positive result was confirmed and is presented here.

## 2. Experimental procedures

Coatings were prepared by an ion beam assisted

sputtering deposition system which was equipped with two Kaufman ion sources used for sputtering deposition and assistant bombardment, respectively(**Fig.1**). The main chamber was evacuated by a turbo molecular pump supported by a booster-rotary pump combination to get a base pressure of $1\times10^{-5}$ Pa. Composite Ti-B-N coatings were synthesized by sputtering a $TiB_2$ target with an argon ion beam while bombarded by another nitrogen ion beam. Bombarding energy, density and nitrogen partial pressure were systematically varied to check their effects on the composition, structure and tribological properties. Silicon (100) wafer and mirror-polished high speed steel sheet were used as substrates. The substrates can be cooled at 20°C or heated up to 750°C.
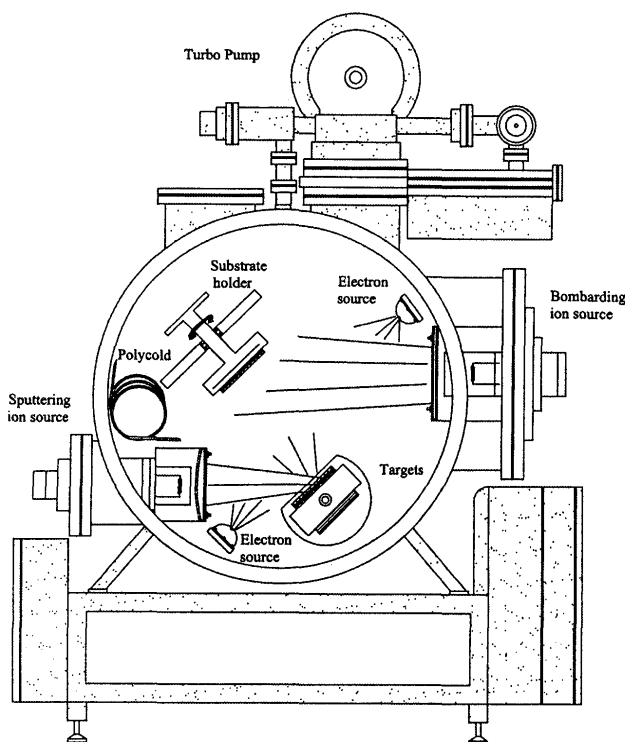


Fig. 1 Schematic of dual ion beam deposition system

Film composition was measured by electron probe microanalysis(EPMA) using a JXA-8600(JEOL) system. Structural characterization was performed by a JDX-3530M x-ray diffractometer (JEOL) with Cu Ka irradiation. FTIR spectroscopy was employed to identify the BN phase by a Nicolet FTIR spectroscopy. Film hardness was evaluated using a Triboscope (Hysitron Inc.) nanoindention system which was interfaced with an atomic force microscope (NanoscopeIII, Digital Instruments). Friction and wear properties were investigated by a ball-on-disk tribometer with a mirror-polished steel ball counterface(diameter 6mm) under room temperature and 40% relative humidity. Normal loads of 1N and 5N were used and the maximum

Hertzian contact pressures were approximately 0.7 and 1.1GPa, respectively. The velocity was maintained at 0.1m/s.

### 3. Results and Discussion
#### 3.1 Composition and Structure

Ti-B-N materials can consist of several phases depending on their composition [9]. The chemical composition of films studied in this work was found to have a constant B/Ti ratio(~2) and different nitrogen concentration. This is not surprising since the films were synthesized by sputtering the $TiB_2$ target and the addition of nitrogen did not change the B/Ti ratio. While the B/Ti ratio remained constant, the nitrogen concentration was found to depend mainly on the nitrogen partial pressure. The nitrogen concentration of TiBN films increased with increasing nitrogen feeding rate. But the nitrogen concentration seems to saturate when the nitrogen feeding rate increases to >15sccm. In this work, bombarding energy and ion-to-atom ratio were found to have little influence on the film composition.
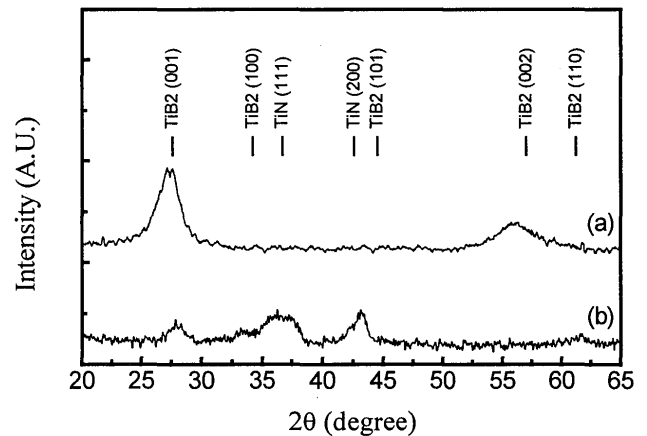


Fig. 2 X-ray diffraction profiles of (a)$TiB_2$ film and (b) TiBN film

According to the Ti-B-N phase diagram [9], the films studied in this work should comprise $TiB_2$, TiN and BN phases. This was proved by structural analysis. **Figure 2** shows the X-ray diffraction profiles of pure $TiB_2$ film and a Ti-B-N film. The pure $TiB_2$ film was obtained by direct sputtering of sintered $TiB_2$ target while the Ti-B-N film was synthesized with additional nitrogen bombardment at 800eV. It is clear that when nitrogen was introduced, an fcc TiN phase was formed. This is in agreement with other work on sputtered Ti-B-N films. [10-13] In addition, the strong (001) texture of $TiB_2$, which is also common in the literature [10-13], was changed to a mixed orientation.

Though reactive sputtered Ti-B-N films have been mainly reported as amorphous [13-15], it was found that films in this work were partly crystalline, as demonstrated by **Fig.2(b)**. From the peak broadening, the

grain size of $TiB_2$ and TiN was calculated to be some tens nanometers. The irregularity of peak shape is attributed to the overlap of peaks from $TiB_2$ and TiN. The low intensities can be explained by the formation of smaller grains together with a relatively large amount of disordered grain boundary materials.
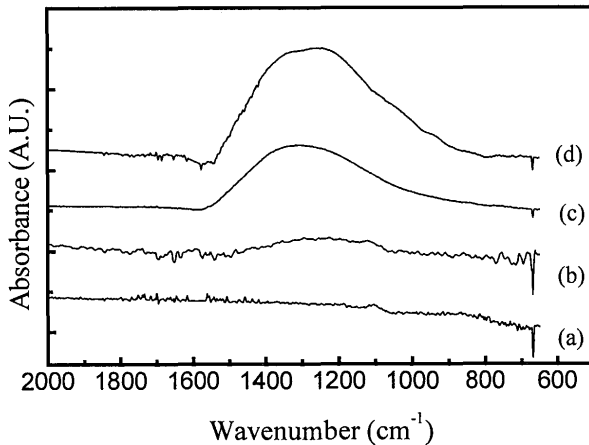


Fig. 3   FTIR spectra of Ti-B-N films synthesized with different nitrogen feed rates: (a) no nitrogen, (b) 5sccm, (c) 10sccm and (d) 15sccm.

While Ti-N and Ti-B bondings were confirmed, there were no traces of any B-N structures in the X-ray diffraction profiles. However, FTIR analysis indicated that B-N bondings exist in the films. **Figure 3** shows the FTIR spectra for pure $TiB_2$ and Ti-B-N films. It can be seen that when nitrogen is introduced, a broad absorption band emerges. With increasing nitrogen feeding rate, the absorption becomes stronger. This implies that B-N bondings were formed in the Ti-B-N films. But it should be noted that the absorption band is centered around $1280cm^{-1}$ which does not coincide with the characteristic absorption bands of h-BN or c-BN(B-N-B bending of h-BN:$800cm^{-1}$, reststrahlen band of c-BN: $1050cm^{-1}$; B-N stretching of h-BN: $1350cm^{-1}$) [16]. This is probably due to the terminating of B-N bondings by titanium atoms. Considering that no B-N peak was detectable in the XRD, we may suspect that B-N bondings were localized within the gaps among $TiB_2$ and TiN crystallites. Consequently, the Ti-B-N films should have a structure such that nanosized $TiB_2$ and TiN crystallites are dispersed in a very thin layer matrix of hexagonal BN.

## 3.2 Tribological properties

Figure 4(a) shows the nanoindentation hardness of the Ti-B-N films versus the nitrogen feeding rate. The zero feeding rate represents a pure $TiB_2$ film. It can be seen that the introduction of nitrogen results in a sharp drop of the film hardness. With increasing nitrogen feeding rate, the film hardness steadily goes down. This

behavior was generally observed for sputtered Ti-B-N films [10-13]. It is attributed to the formation of soft phase of hexagonal B-N.
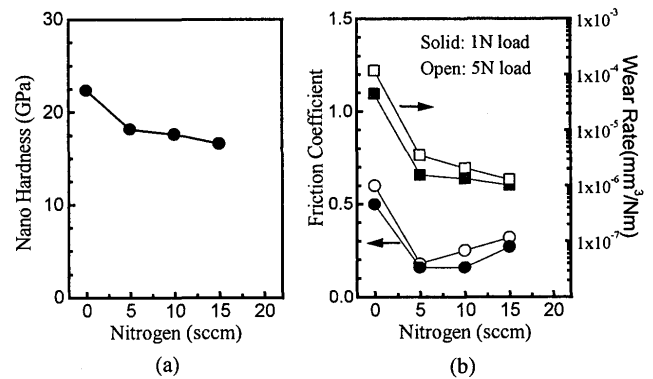


Fig. 4   (a) Nanoindentation hardness, (b) friction coefficient and wear rate of Ti-B-N films synthesized with different nitrogen feed rates.

In this work, Ti-B-N films were found to exhibit better tribological properties than pure $TiB_2$. As illustrated by **Fig. 4(b)**, the coefficient of friction and wear rate of Ti-B-N films were both found smaller than those of pure $TiB_2$. In particular, the wear rate of Ti-B-N films was more than one order smaller than that of pure $TiB_2$. Ti-B-N films also displayed higher load-bearing capacity which is suggested by the less difference between wear rates under small load(1N) and high load (5N). This wear-resistance improvement can be explained by the formation of hexagonal BN. The lamellar nature of h-BN makes it easy to deform under external stress so that stress concentration imposed by the wear counterface can be relaxed and severe wear failure of the film (a crack, for example) is prohibited. This mechanism was confirmed by the observation that there was much less debris on the wear track of Ti-B-N films than pure $TiB_2$ films. Another factor which contributes to the wear-resistance improvement of Ti-B-N films is their smaller friction coefficients(**Fig.4(b)**), though the friction coefficient displayed a slight increase over the nitrogen feeding rate. The decrease of friction coefficient may also come from the lamellar nature of h-BN. But it should be mentioned that this is different from magnetron sputtered Ti-B-N films which were reported to have rather high friction coefficients [8,9]. It is believed that experimental parameters played a key role in this case.

The ion/atom transport ratio was found to have no evident influence on the film friction coefficient, neither on the film hardness and anti-wear performance. For example, when the bombarding energy was fixed at 50eV and nitrogen feeding rate was maintained at 15sccm, the film hardness, friction coefficient and wear rate were approximately constant at 12GPa, 0.2 and $1x10^{-6}mm^3/mN$, respectively, though the ion/atom ratio was varied from unity to eight. On the contrary, substrate temperature

showed a great influence on the film hardness. As shown in **Fig.5**, the hardness of TiBN films decreased with increasing temperature at elevated substrate temperatures. This could be attributed to the easy formation of h-BN since h-BN is a thermodynamic stable phase under the present experimental condition. However, when the film growth temperature was reduced down to 20°C, the film hardness was only about 12GPa. As a whole, the film hardness showed a maximum around a substrate temperature of about 100°C.
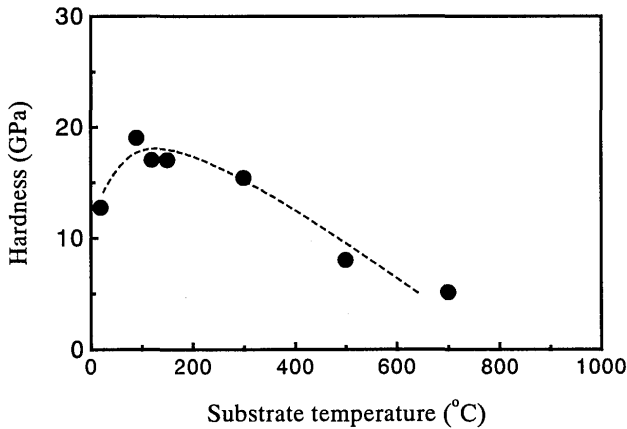


**Fig. 5** Nanoindentation hardness of Ti-B-N films synthesized under different substrate temperatures (N2 feed rate: 15sccm, bombarding energy: 350eV, ion/atom ratio: 1).

Bombarding energy was also found to have a significant influence on the properties of the Ti-B-N film. As shown by **Fig.6(a)**, the hardness of Ti-B-N films first increases with the energy of bombarding nitrogen ions and then decreases with further increase of the bombarding energy. This results in a hardness maximum around 400eV. It should be noted that the hardness maximum is still smaller than the hardness of pure $TiB_2$ film. The friction coefficient showed a similar behavior(**Fig.6(b)**). A peak value arises when the bombarding energy is around 400eV. However, all these Ti-B-N films exhibit smaller friction coefficients compared with pure $TiB_2$ film (**Fig.6(b)**). Furthermore, the friction coefficients are more load-independent (compare **Fig.6** with **Fig.4**), which may imply that the Ti-B-N films have larger load-bearing capacity.

The influence of bombarding energy on wear resistance of Ti-B-N films is also shown in **Fig.6(b)**. The most interesting feature is that the wear rate can be significantly lowered when the bombarding energy is about 150eV. Also, films synthesized under this condition displayed higher load-bearing capacities. When the normal load was increased from 1N to 5N, the wear rate remained almost the same. The measured wear rate for these Ti-B-N films was about two orders smaller than that of pure $TiB_2$ film. This can be explained by the

combination of a mild hardness, a smaller friction coefficient and an improved toughness which can inferred from the structural analysis in the previous section. Since wear resistance is influenced by many material characteristics such as hardness, toughness, friction coefficient, and so on, an enhancement resulting from the optimization of these properties should be reasonable. This idea was demonstrated by the present study. The improved anti-wear performance of Ti-B-N films was believed to come from an optimal configuration of hard phases($TiB_2$ and TiN) and soft lubricating phase(h-BN).
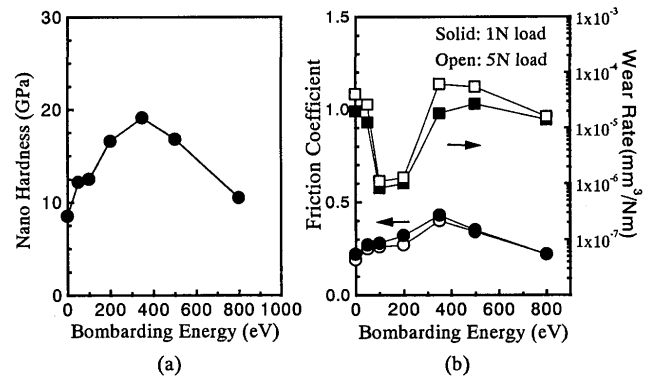


**Fig. 6** (a) Nanoindentation hardness, (b) friction coefficient and wear rate of Ti-B-N films synthesized with different bombarding energies.

From the structural analysis, the Ti-B-N films studied in this work were proved to have a composite structure such that nanosized $TiB_2$ and TiN crystallites were dispersed in a thin layer matrix of hexagonal BN. Therefore, the optimal microstructure for good wear-resistance should involve appropriate size and amount of $TiB_2$ and TiN crystallites together with proper "binding" of the BN matrix. Further work is still in process to correlate these structural features to experimental parameters.

## 4. Conclusions

Ti-B-N films were synthesized by nitrogen-ion-beam-assisted sputtering deposition of $TiB_2$. The film composition was found to have a fixed B/Ti ratio (approximately 2) and the nitrogen concentration depended mainly on the nitrogen feeding rate. Structural analysis revealed that the Ti-B-N films had a nanocomposite structure comprising nanosized $TiB_2$ and TiN crystallites and a thin layer matrix of hexagonal BN.

While the hardness of Ti-B-N films generally decreased compared with pure $TiB_2$, improved tribological properties were observed. Contrary to the magnetron sputtered Ti-B-N films [8,9], a smaller friction coefficient (~0.2) was confirmed for some Ti-B-N films in this study. The substrate temperature and bombarding energy of nitrogen ions were found to have a great influence on the film properties, though little effect on

the film composition. When the bombarding energy was around 150eV and the substrate temperature was around 100°C, the wear rate of Ti-B-N film was two orders lower than that of pure $TiB_2$ film. Also, films synthesized under this condition displayed higher load-bearing capacities. This wear-resistance improvement was explained by an optimization with hardness, toughness and friction coefficient, which came from an optimal nano-sized configuration of hard phases ($TiB_2$ and TiN) and soft lubricating phase (h-BN).

## References

1) R. Gilmore, M.A. Baker, P.N. Gibson, W. Gissler, Surf. Coat. Technol. 105 (1998) 45
2) A. Savan, E. Pfluger, R. Goller, W. Gissler, Surf. Coat. Technol. 126 (2000) 159
3) J. Musil, P. Zeman, H. Hruby, P.H. Mayrhofer, Surf. Coat. Tech., 120-121 (1999) 179
4) S. Veprek, J. Vac. Sci. Technol. A 17(1999) 2401
5) E.R. Braithwaite, Solid Lubricants and Surfaces, Pergamon (1964) 199
6) A.J. Haltner, Sliding behavior of some layer lattice compounds in ultrahigh vacuum, ASLE Trans. 9 (1966) 136
7) Yoshitsugu Kimura, T. Wakabayashi, K. Okada, T. Wada, H. Nishikawa, Wear, 232 (1999) 199
8) W. Herr, B. Matthes, E. Broszeit, K.H. Kloos, Mater. Sci. Eng., A 140 (1991) 616
9) T.P. Mollart, J. Haupt, R. Gilmore, W. Gissler, Surf. Coat. Technol., 86-87(1996) 231
10) C. Mitterer, P. Rodhammer, H. Stori, F. Jeglitsch, J. Vac. Sci Technol. A 7 (1989) 2646
11) P. Losbichler, C. Mitterer, Surf. Coat. Technol, 97 (1997) 568
12) C. Mitterer, P. Losbichler, F. Hofer, P. Warbichler, P.N. Gibson and W. Gissler, Vacuum, 50 (1998) 313
13) R.Wiedemann, V. Weihnacht, H. Oettel, Surf. Coat. Technol., 116-119 (1999) 302
14) L. Chaleix, J. Machet, Surf. Coat. Technol, 91 (1997) 74
15) H. Deng, J. Chen, R.B. Inturi, J.A. Barnard, Surf. Coat. Technol., 76-77 (1995) 609
16) Y. Kusano, J.E. Evetts, I.M. Hutching, Thin Solid Films, 343 (1999) 250